

# Viscous control of shallow elastic fracture

Tim Large<sup>1</sup>, John Lister<sup>2</sup>, and Dominic Skinner<sup>2</sup>

<sup>1</sup>M.I.T., USA

<sup>2</sup>Department of Applied Mathematics and Theoretical Physics, University of Cambridge, UK

(Received xx; revised xx; accepted xx)

This paper considers the problem of a semi-infinite crack parallel to the boundary of a half plane, with the crack filled by an incompressible viscous fluid. The dynamics are driven by a bending moment applied to the arm of the crack, and we look for travelling wave solutions. We examine two models of fracture; fracture with a single tip, and fracture with a wet tip preceded by a region of dry fracture.

**Key words:** Authors should not enter keywords on the manuscript, as these must be chosen by the author during the online submission process and will then be added during the typesetting process (see <http://journals.cambridge.org/data/relatedlink/jfm-keywords.pdf> for the full list)

## 1. Introduction

Here we review the literature as well as describe the problem in more detail. We have the vertical displacement  $h$ , the horizontal displacement  $g$ , the thickness of the arm  $l$ , and the pressure  $p$ . We look for a travelling wave solution (propagating left), with speed  $c$ .

## 2. Formulation of problem

From lubrication, we have Poiseuille flow in the crack. We obtain the flux, and conservation of mass as

$$q = -\frac{1}{12\mu} \frac{dp}{dx} h^3, \quad \frac{\partial q}{\partial x} + \frac{\partial h}{\partial t} = 0, \quad (2.1)$$

which combined gives

$$\frac{dp}{dx} = 12\mu c/h^2. \quad (2.2)$$

Setting  $p \rightarrow 0$  at  $x \rightarrow \infty$ , we can write this in integral form,

$$p(x) = - \int_x^\infty 12\mu c/h(\tilde{x})^2 d\tilde{x}. \quad (2.3)$$

From the linear theory of elasticity, due to others who have studied this problem, we have

$$\begin{bmatrix} -\sigma_y \\ -\tau_{xy} \end{bmatrix} = \begin{bmatrix} p(x) \\ 0 \end{bmatrix} = \frac{1}{l} \int_0^\infty \boldsymbol{\kappa} \left( \frac{\tilde{x} - x}{l} \right) \begin{bmatrix} g'(\tilde{x}) \\ h'(\tilde{x}) \end{bmatrix} d\tilde{x}, \quad (2.4)$$

where the integral kernel is

$$\mathbf{K}(\xi) = \begin{bmatrix} K_{11} & K_{12} \\ K_{21} & K_{22} \end{bmatrix} = \begin{bmatrix} \frac{(32-24\xi^2)}{(\xi^2+4)^3} & \frac{(48\xi^2-64)}{\xi(\xi^2+4)^3} \\ -\frac{(16\xi^4+16\xi^2+4)}{\xi(\xi^2+4)^3} & -\frac{(32-24\xi^2)}{(\xi^2+4)^3} \end{bmatrix}. \quad (2.5)$$

The boundary conditions near  $x = 0$  are governed by fracture mechanics

$$K_I = \lim_{x \rightarrow 0} \frac{E}{1-\nu^2} \sqrt{\frac{\pi}{8}} \sqrt{x} h'(x), \quad K_{II} = \lim_{x \rightarrow 0} \frac{E}{1-\nu^2} \sqrt{\frac{\pi}{8}} \sqrt{x} g'(x). \quad (2.6a, b)$$

As we go to  $x \gg l$ , we are looking at the problem of peeling off a thin strip from an elastic half space. We can then use beam theory approximations, which give

$$M(x) = \frac{El^3}{12(1-\nu^2)} \frac{d^2 h}{dx^2} = \frac{El^3}{6(1-\nu^2)} \frac{dg}{dx}, \quad p = \frac{El^3}{12(1-\nu^2)} h^{(4)}(x) \quad (2.7a, b)$$

As  $x \rightarrow \infty$ ,  $M(x) \rightarrow M$ , the applied bending moment, so this gives us boundary conditions on  $h''$ ,  $g'$ .

### 2.1. Rescaling

We can define the following dimensionless variables

$$x = l\xi, \quad h(x) = \frac{12M(1-\nu^2)}{El} H(\xi), \quad g(x) = \frac{12M(1-\nu^2)}{El} G(\xi), \quad (2.8)$$

$$p = \frac{3M}{\pi l^2} \Pi(\xi), \quad K_I = Ml^{-3/2} \kappa_I, \quad K_{II} = Ml^{-3/2} \kappa_{II}, \quad \lambda = \frac{4\pi\mu p^* l^3}{M^2}. \quad (2.9)$$

With these scalings, the equations become

$$\begin{bmatrix} \Pi \\ 0 \end{bmatrix} = \int_0^\infty \mathbf{K}(\xi - \tilde{\xi}) \begin{bmatrix} G'(\tilde{\xi}) \\ H'(\tilde{\xi}) \end{bmatrix} d\tilde{\xi} \quad (2.10)$$

$$H^2 \frac{d\Pi}{d\xi} = \lambda \quad \text{or} \quad \Pi(\xi) = - \int_\xi^\infty \lambda / H(\tilde{\xi})^2 d\tilde{\xi} \quad (2.11a, b)$$

$$\lim_{\xi \rightarrow \infty} H'' = 1, \quad \lim_{\xi \rightarrow \infty} G' = \frac{1}{2}, \quad \lim_{\xi \rightarrow 0} 3\sqrt{2\pi\xi} H' = \kappa_I, \quad \lim_{\xi \rightarrow 0} 3\sqrt{2\pi\xi} G' = \kappa_{II}, \quad (2.12)$$

These shall be the governing equations for the rest of this paper.

The equations of the linear perturbation problem:

$$\Pi = \Pi_0 + \mathcal{E}\Pi_1 + O(\mathcal{E}), \quad H = H_0 + \mathcal{E}H_1 + O(\mathcal{E}) \quad (2.13)$$

$$\begin{bmatrix} \Pi_1 \\ 0 \end{bmatrix} = \int_0^\infty \mathbf{K}(\xi - \tilde{\xi}) \begin{bmatrix} G'_1(\tilde{\xi}) \\ H'_1(\tilde{\xi}) \end{bmatrix} d\tilde{\xi}, \quad H_0^2 \Pi'_1 + 2H_0 H_1 \Pi'_0 = \lambda_1 \quad (2.14a, b)$$

$$H_1'' \rightarrow 0 \text{ as } \xi \rightarrow \infty, \quad H_1 \sim \xi^s + \frac{\tilde{A}\lambda_1}{3\lambda_0^{2/3}} \xi^{2/3} + \dots \text{ as } \xi \rightarrow 0 \quad (2.15a, b)$$

But these can be made into a more convenient form, by considering instead  $\tilde{\Pi} = \Pi_0 - 3\lambda_0/\lambda_1 \Pi_1$ , and similar for  $\tilde{H}$ ,  $\tilde{G}$ . The equations become

$$\begin{bmatrix} \tilde{\Pi} \\ 0 \end{bmatrix} = \int_0^\infty \mathbf{K}(\xi - \tilde{\xi}) \begin{bmatrix} \tilde{G}'(\tilde{\xi}) \\ \tilde{H}'(\tilde{\xi}) \end{bmatrix} d\tilde{\xi}, \quad H_0^2 \tilde{\Pi}' + 2H_0 \tilde{H} \Pi'_0 = 0 \quad (2.16a, b)$$

$$\tilde{H}'' \rightarrow 1 \text{ as } \xi \rightarrow \infty, \quad \tilde{H} \sim -\frac{3\lambda_0}{\lambda_1}\xi^s + \dots \text{ as } \xi \rightarrow 0 \quad (2.17a, b)$$

These are the equations for the two tip problem

$$\begin{bmatrix} \Pi \\ 0 \end{bmatrix} = \int_{-L}^{\infty} \mathbf{K}(\tilde{\xi} - \xi) \begin{bmatrix} G'(\tilde{\xi}) \\ H'(\tilde{\xi}) \end{bmatrix} d\tilde{\xi}, \quad \Pi = \int_{\xi}^{\infty} \lambda/H(\tilde{\xi})^2 d\tilde{\xi} \quad (2.18a, b)$$

$$\lim_{\xi \rightarrow \infty} H'' = 1, \quad \lim_{\xi \rightarrow \infty} G' = \frac{1}{2} \quad (2.19a, b)$$

$$\lim_{\xi \rightarrow 0} 3\sqrt{2\pi\xi}H' = 0, \quad \lim_{\xi \rightarrow -L} 3\sqrt{2\pi\xi}G' = \kappa_{II} \quad (2.20a, b)$$

### 3. Numerical scheme

#### 3.1. Single Tip

We discretize the problem by taking  $n+1$  points  $\boldsymbol{\xi} = (\xi_0 = 0, \xi_1, \dots, \xi_n)$  at which we measure  $H'$ ,  $G'$ , and  $n$  intermediate points  $\boldsymbol{\zeta} = (\zeta_0, \dots, \zeta_{n-1})$  at which to measure  $\Pi$ , so that  $\xi_0 < \zeta_0 < \dots < \zeta_{n-1} < \xi_n$ . We work with  $\sqrt{\xi}G'(\xi)$ ,  $\sqrt{\xi}H'(\xi)$  near the tip to avoid singularities. We define  $\boldsymbol{\theta}_G = [\sqrt{\xi_0}G'(\xi_0), \dots, \sqrt{\xi_{t-1}}G'(\xi_{t-1}), G'(\xi_t), \dots, G'(\xi_n)]$ ,  $\boldsymbol{\theta}_H = [\sqrt{\xi_0}H'(\xi_0), \dots, \sqrt{\xi_{t-1}}H'(\xi_{t-1}), H'(\xi_t), \dots, H'(\xi_n)]$ , as well as  $\boldsymbol{\theta} = [\boldsymbol{\theta}_G, \boldsymbol{\theta}_H]$ , (where  $\sqrt{\xi_0}G'(\xi_0) = \lim_{\xi \rightarrow \xi_0} \sqrt{\xi}G'(\xi)$ ). Typically  $t \approx n/2$  was used. The elasticity integral is linear in  $G'$ ,  $H'$ , and so the discretized integration is linear in  $\boldsymbol{\theta}$ . Such a linear relation may be written as

$$[\Pi(\zeta_1), \dots, \Pi(\zeta_{n-1}), \underbrace{0, \dots, 0}_{n-1}] = \mathbf{J}\boldsymbol{\theta}. \quad (3.1)$$

By imposing  $H(0) = 0$ , and choosing a sensible interpolation, one can recover  $H(\xi_i)$  from  $\boldsymbol{\theta}_H$ . Therefore, from the lubrication integral, there exists another expression for  $[\Pi(\zeta_0), \dots, \Pi(\zeta_{n-1})]$  as some function of  $\boldsymbol{\theta}_H$ . So we can write

$$[\Pi(\zeta_1), \dots, \Pi(\zeta_{n-1}), \underbrace{0, \dots, 0}_{n-1}] = \mathbf{J}\boldsymbol{\theta} = \mathbf{f}(\boldsymbol{\theta}_H), \quad (3.2)$$

for some function  $\mathbf{f}$ .

Both  $G'(\xi_n)$ , and  $H''(\xi_n)$  are known from our beam theory asymptotic expansion. But these are linear in  $\boldsymbol{\theta}$ , as  $G'(\xi_n) = \theta_n$ , and  $H''(\xi_n) \approx (\theta_{2n} - \theta_{2n-1})/(\xi_n - \xi_{n-1})$ . Therefore we can add another two rows to  $\mathbf{J}$ , so that

$$\mathbf{A}\boldsymbol{\theta} = [\mathbf{f}(\boldsymbol{\theta}), G'(\xi_n), H''(\xi_n)]. \quad (3.3)$$

Where the  $\mathbf{A}$  is the enlarged matrix. This can be solved by Newton's method from quite arbitrary initial guesses.

For  $\xi_i < \xi < \xi_{i+1}$ , we interpolate as

$$G'(\xi) = \begin{cases} \xi^{-1/2}(a_i\xi + b_i) \\ a_i\xi + b_i \end{cases}, \quad H'(\xi) = \begin{cases} \xi^{-1/2}(c_i\xi^{1/2} + d_i) \\ c_i\xi + d_i \end{cases}, \quad \text{for } \begin{cases} i < t \\ i \geq t \end{cases} \quad (3.4)$$

The choice of interpolating function was based on the appearance of the relevant functions. We will also define  $a_n, b_n, c_n, d_n$  for interpolation beyond  $\xi_n$ . With this choice of interpolation, there exist exact closed form expressions for both the lubrication integral, and the elasticity integral, in terms of the  $a_i - d_i$  coefficients.

We therefore want to determine  $a_i - d_i$  in terms of  $\boldsymbol{\theta}$ . Continuity of  $G'$ ,  $H'$  imposes  $2(n-1)$  equations. For  $G'$  they are

$$\begin{aligned} a_i \xi_{i+1} + b_i &= a_{i+1} \xi_{i+1} + b_{i+1} = \theta_{i+1}, \text{ for } i < n, i \neq t-1 \\ \xi^{-1/2}(a_{t-1} \xi_t + b_{t-1}) &= a_t \xi_t + b_t = \theta_t, \end{aligned} \quad (3.5)$$

with similar equations for  $H'$  (accounting for the slightly different interpolation). We also have the  $2n$  equations following from the definition of  $\boldsymbol{\theta}$ , such as  $a_i \xi_i + b_i = \theta_i$  for  $t \leq i \leq n$ .

From our asymptotic expansion (via beam theory) we know  $\theta_n = G'(\xi_n)$  and  $a_n = G''(\xi_n)$ . Therefore we can write

$$a_n = \frac{G''(\xi_n)}{G'(\xi_n)} \theta_n, \quad b_n = \theta_n - a_n \xi_n = \left(1 - \frac{G''(\xi_n)}{G'(\xi_n)}\right) \theta_n \quad (3.6)$$

With  $H$ , we know that  $c_n = H''(\xi_n)$ ,  $c_{n-1} = H''(\xi_{n-1})$ , and so we have that

$$c_n = \frac{H''(\xi_n)}{H''(\xi_{n-1})} c_{n-1}, \quad d_n = -c_n \xi_n + c_{n-1} \xi_n + d_{n-1} \quad (3.7)$$

Therefore, we have enough equations to calculate a matrix  $\mathbf{T}$ , so that

$$[a_1, \dots, a_n, b_1, \dots, b_n, c_1, \dots, c_n, d_1, \dots, d_n] = \mathbf{T} \boldsymbol{\theta} \quad (3.8)$$

Note that we choose a value of  $\lambda$ , fix the boundary conditions at  $\xi \rightarrow \infty$ , then solve the problem and subsequently recover the boundary conditions at  $\xi = 0$  ( $\kappa_I$ ,  $\kappa_{II}$ ). This can then be inverted, so that we think of  $\lambda = \lambda(\kappa_I)$ . Physically, we know  $\kappa_I$ , and want to find  $\lambda$ , but in numerically solving the problem, it makes more sense to choose  $\lambda$  and recover  $\kappa_I$ .

The spacing of the points should reflect that the important part of the problem is happening near the tip, and this is where the points should be concentrated. The spacing that was typically used in numerical calculations was

$$\xi_i = \tan^2(\chi i/m), \quad i = 1, \dots, m < n \quad (3.9)$$

where  $\chi$  is chosen so that  $\tan^2(\chi) = O(10)$ , and the remaining points are added in a geometric progression, so that

$$\xi_{i+1} = (\xi_m/\xi_{m-1}) \xi_i, \quad i = m, \dots, n-1 \quad (3.10)$$

### 3.2. Linear Perturbation Problem

From equation 2.17b, we anticipate a singularity of the form  $\xi^{s-1}$  in  $\tilde{H}'$ , (we still expect a  $\xi^{-1/2}$  singularity in  $\tilde{G}'$ ). Therefore, the interpolation used is

$$\tilde{G}'(\xi) = \begin{cases} \xi^{-1/2}(a_i \xi + b_i) \\ a_i \xi + b_i \end{cases}, \quad \tilde{H}'(\xi) = \begin{cases} \xi^{s-1}(c_i \xi + d_i) \\ c_i \xi + d_i \end{cases}, \quad \text{for } \begin{cases} i < t \\ i \geq t \end{cases} \quad (3.11)$$

Some of the integrals no longer have exact expressions. In this case, they are calculated by a numerical integration routine. We define  $\tilde{\boldsymbol{\theta}}$  to be like  $\boldsymbol{\theta}$ , but with  $\tilde{H}'$ ,  $\tilde{G}'$  instead of  $H$ ,  $G$ .

The lubrication equation for the linear perturbation problem (2.16b) may be written as

$$\tilde{H}(\zeta) = \int_{\zeta}^{\infty} \frac{2\lambda_0 \tilde{H}}{H_0^3} d\xi. \quad (3.12)$$

This is linear in  $\tilde{H}$ , and so in  $\tilde{\theta}$ . The integrals that appear were determined numerically. We end up with a matrix  $\mathbf{R}$ , such that

$$[\tilde{H}(\zeta_1), \dots, \tilde{H}(\zeta_{n-1})] = \mathbf{R}\tilde{\theta} \quad (3.13)$$

Padding out  $\mathbf{R}$  with zeros, until it is of size  $2n \times 2n$ , we see that

$$\left( \mathbf{A} - \begin{bmatrix} \mathbf{R} \\ \mathbf{0} \end{bmatrix} \right) \boldsymbol{\theta} = [0, \dots, 0, \tilde{G}'(\xi_n), \tilde{H}''(\xi_n)] \quad (3.14)$$

Since we haven't changed the integral kernel, the beam theory asymptotics remain the same, and together with 3.12, we can calculate an asymptotic expression for  $\tilde{H}''(\xi_n)$ ,  $\tilde{G}'(\xi_n)$ . Here, we do not need to deploy Newton's method, as we can simply solve the linear set of equations, 3.14.

### 3.3. Double Tip

In solving the problem of two tips situated at  $-L$  and  $0$ , it is given that  $H = 0$  for  $\xi < 0$ , and thus  $H' = 0$  for  $\xi < 0$ . We take  $n$  points to cover  $0 \leq \xi < \infty$ , and  $r$  points to cover  $-L \leq \xi < 0$ . we label these points so that

$$\boldsymbol{\xi} = [\xi_{-r} = -L, \xi_{1-r}, \dots, \xi_0 = 0, \xi_1, \dots, \xi_n]. \quad (3.15)$$

We interpolate  $G'$  expecting a  $\xi^{-1/2}$  singularity at  $\xi = -L$ , and  $H'$  expecting a  $\xi^{-1/2}$  singularity at  $\xi = 0$ . We do not calculate  $H$  for  $\xi < 0$  (although it is easily done), but just require that  $\sigma_{xy} = 0$  for  $\xi < 0$ . This provides enough equations for the problem to be solved as before, with Newton's method.

Note that we input  $-L$  and  $\lambda$  and recover  $\kappa_I, \kappa_{II}$ , where  $\kappa_I$  is measured at  $0$ . Physically, for  $L > 0$ , we must have  $\kappa_I = 0$ . Numerically we solve for some  $\lambda, L$ , find  $\kappa_I > 0$  and extrapolate to  $\kappa_I = 0$ .

The spacing of points for  $\xi < 0$  was chosen so that there was a concentration of points near  $-L$  and near  $0$ .

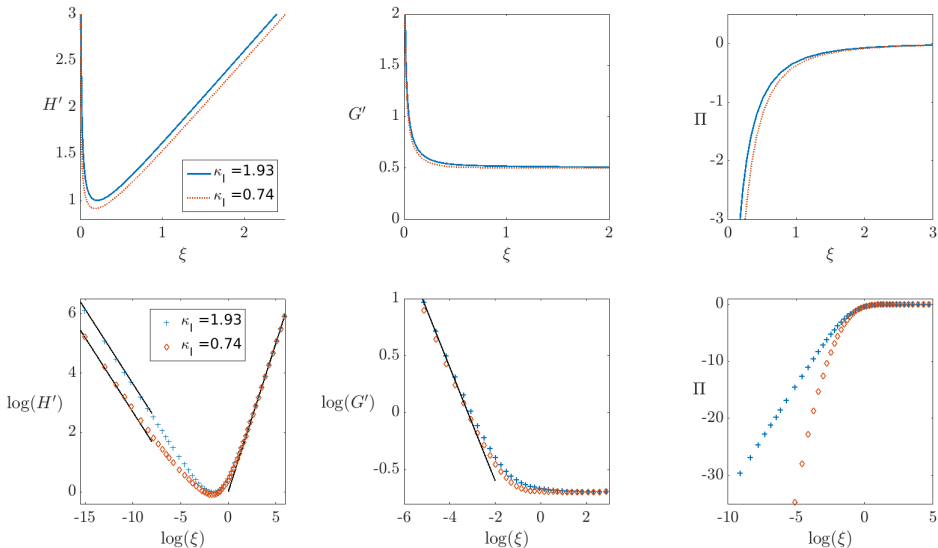


FIGURE 1. Numerical solutions for two typical  $\kappa_I$  values. log-log plots are shown for  $H', G'$ , with solid lines indicating the predicted asymptotics;  $\log(H') \approx -\frac{1}{2}\kappa_I \log(\xi)$ ,  $\log(G') \approx -\frac{1}{2}\kappa_{II} \log(\xi)$  near  $\xi = 0$ , and  $\log(H') \approx \log(\xi)$ ,  $\log(G') \approx -\log(2)$ , as  $\xi \rightarrow \infty$ . Figure produced with  $n = 465$ ,  $x_n = 819$ .

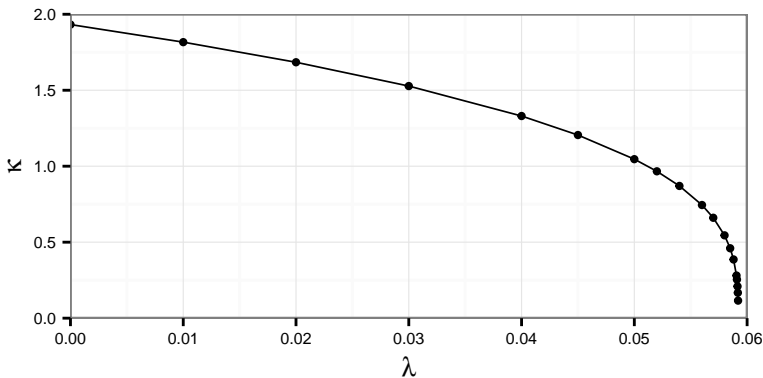


FIGURE 2. Here we vary the parameter  $\lambda$  and plot the change in  $\kappa_I$ . Figure produced with  $n = 465$ ,  $x_n = 819$ .

## 4. Results

### 4.1. Single tip

Start off with some of the basic graphs showing  $H', G'$ , and  $\Pi$  against  $\xi$ .

Obvious questions to ask at this point are: How are you sure this is the right answer, what is the effect of  $n$ ,  $\xi_{\text{end}}$ ? In the next graph, we determine the effect of extending  $\xi_{\text{end}}$ , by adding on extra points (so maintaining the same resolution near the tip). There is a satisfactory demonstration of convergence.

By adding points on in a geometric progression, it becomes quite cheap to extend out to  $\xi_{\text{end}} \approx 800$  or so. Once one has done this, it is apparent that the effect of the tip resolution dominates the effect of finite truncation, as the following figure shows.

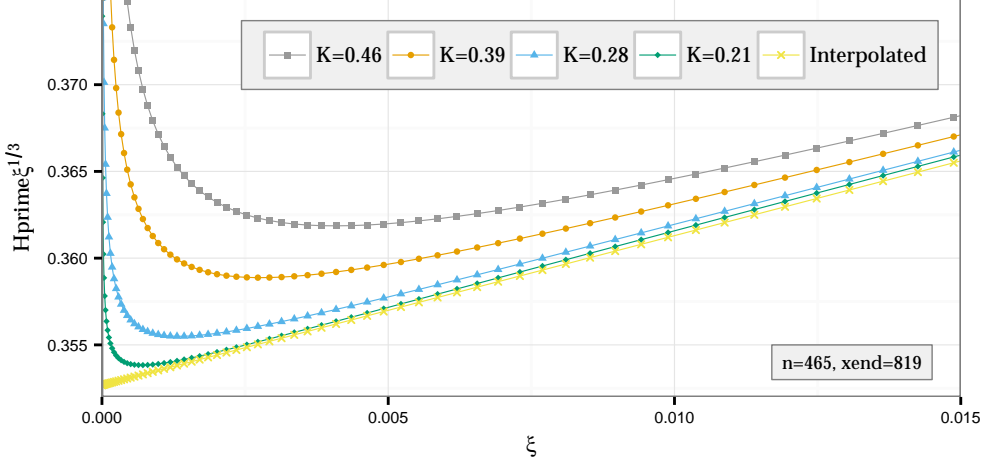


FIGURE 3. As  $\kappa_I \rightarrow 0$ ,  $H'$  moves from a  $\xi^{-1/2}$  singularity to a  $\xi^{-1/3}$  singularity. We can not calculate  $\kappa_I = 0$ , but the extrapolation to it is shown.

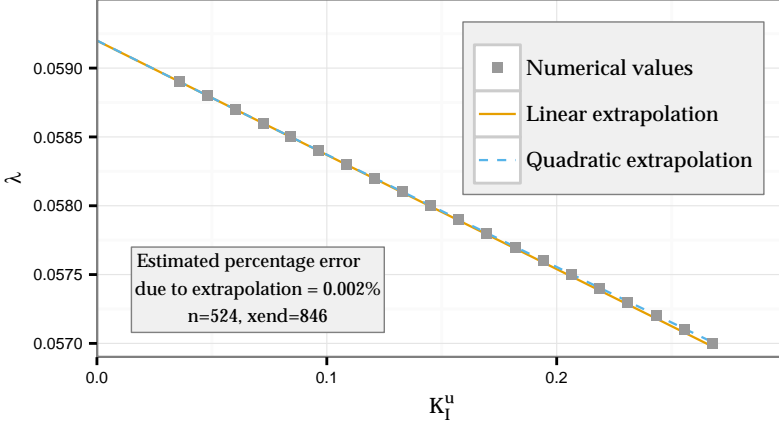


FIGURE 4. A linear fit from the two smallest  $\kappa_I$  values is plotted, as is a quadratic fit from the three smallest  $\kappa_I$  values. They are almost indistinguishable at this scale. The difference between the two extrapolations to  $\kappa_I = 0$ , provides an estimate of the error in calculating  $\lambda_0$ , (not accounting for the error due to  $n$ .)

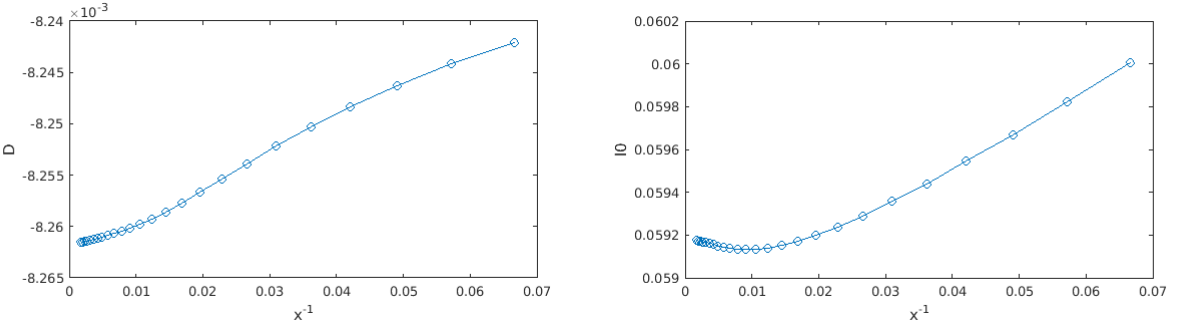


FIGURE 5. As we increase  $\xi_n$ , we can estimate the effect of finite truncation. The figure starts with  $n = 400$ , and increases  $\xi_n$  by adding more points until  $n = 544$ .

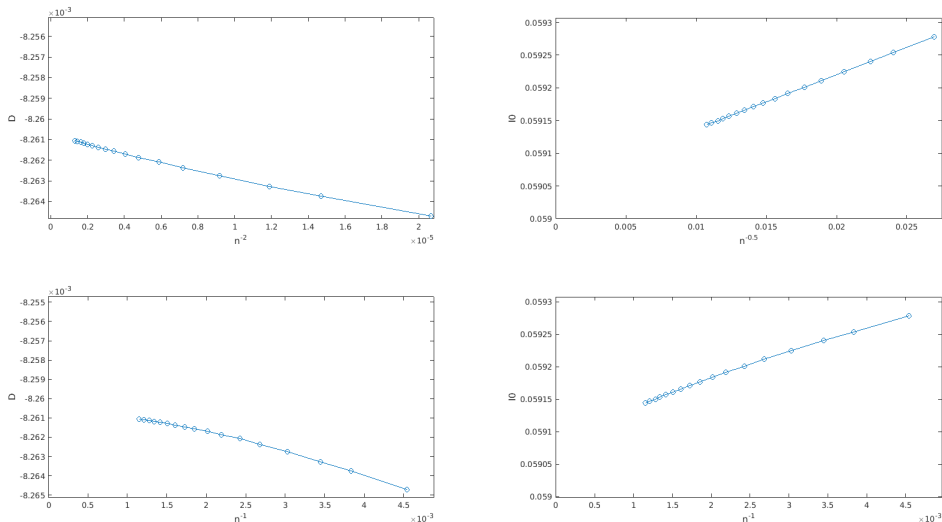


FIGURE 6. Our best guess at  $\lambda_0$  and  $D$ , and the approximate error one can expect in them

By increasing  $n$  (for large  $\xi_{\text{end}}$ ), we have been able to determine  $\lambda_0$  and  $D$

#### 4.2. Linear perturbation problem

We solve the linear perturbation problem. All that we really want to know is that we see the  $\xi^{s-1}$  behaviour that we expect, and we ask what the intercept of  $\tilde{H}_1$  is. It is perhaps worth mentioning the difficulties in measuring the intercept and perhaps a notion of the sensitivity of the result on the estimate provided for  $H_0$ . Illustrating that is the next figure

Then we include the figure that shows convergence with different  $n$  values to something approaching the right answer.

#### 4.3. Two tips

After the linear perturbation problem, we move on to the two tip problem. Perhaps some graphs that show an outline of the full numerical problem with non-zero  $\kappa_I$  and  $\kappa_{II}$ , although these are not physical.

What would be nice, although it doesn't exist yet, is some sort of record of how we now extrapolate to  $\kappa_I = 0$ . This is certainly a plot that needs to be made. We now move on to the  $\kappa_I = 0$  set of relations.

## 5. Discussion

This is where we discuss the figures, possibly include more figures, and draw the results and conclusions of this paper.

Perhaps the first thing worth mentioning is the somewhat contrived, but pretty accurate formulae for  $\lambda$  in terms of  $\kappa_I$ . This holds for any toughness in the single tip case.

Then we could move on to talk about the decoupling between the fluid problem and the dry fracture problem. Relevant graphs to include would show that  $H$  really doesn't



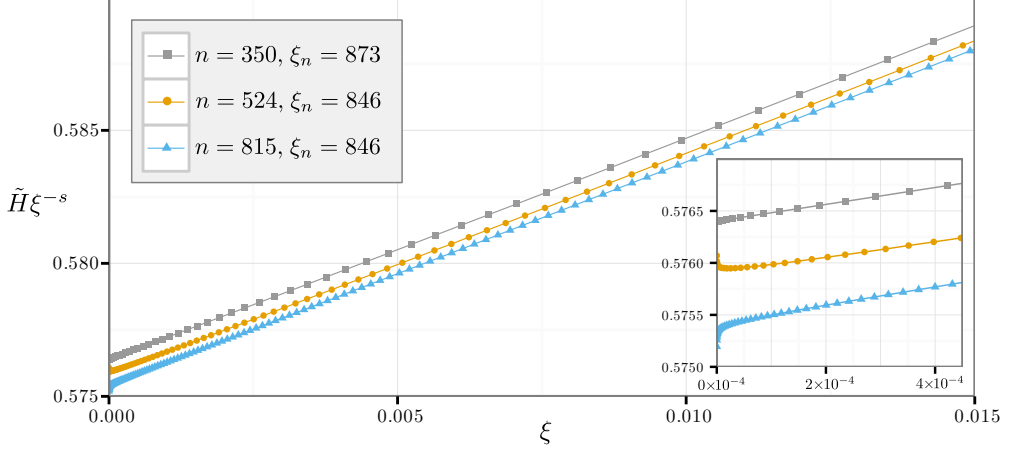


FIGURE 7. The numerical solution of the linear perturbation problem for a selection of resolutions. Of interest is the value of the intercept, which as shown is dependent on the resolution. Also shown is the numerical instability near the tip, due to our difficulty in calculating  $H_0$  for  $\xi \ll 1$ .

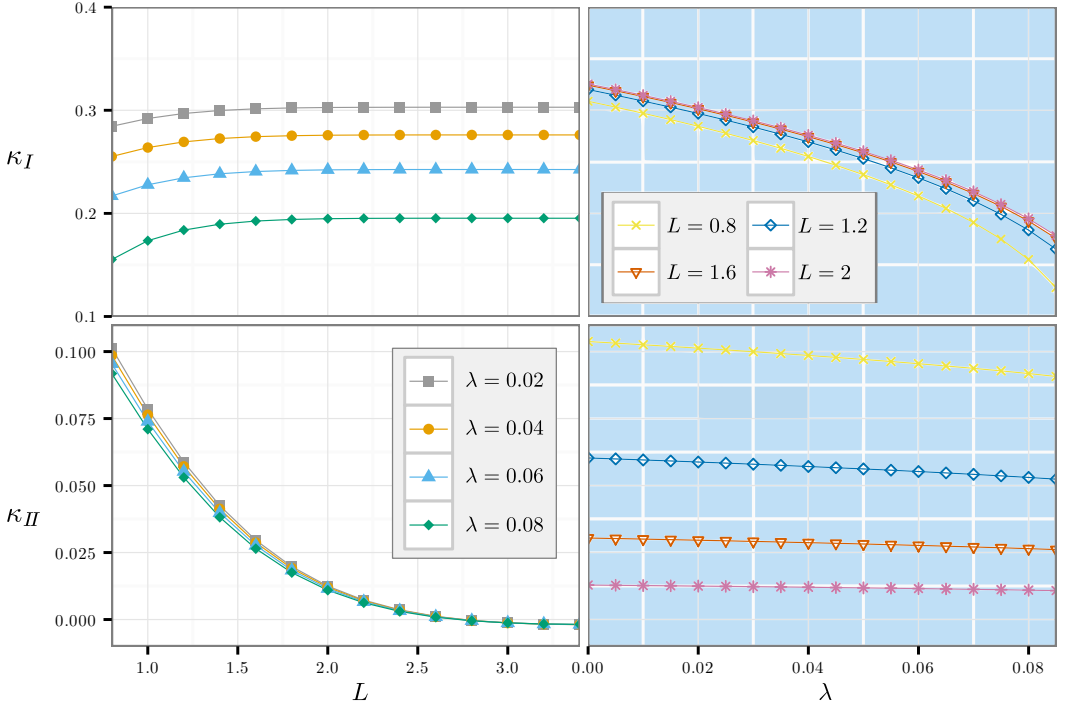
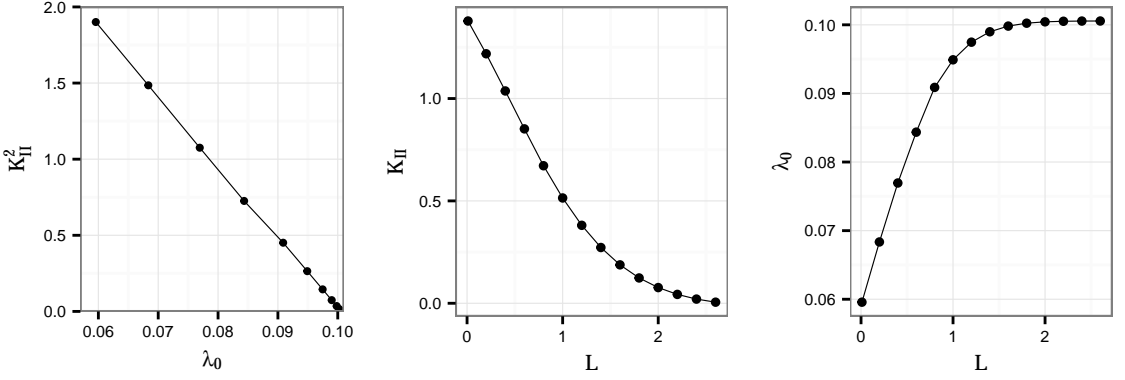
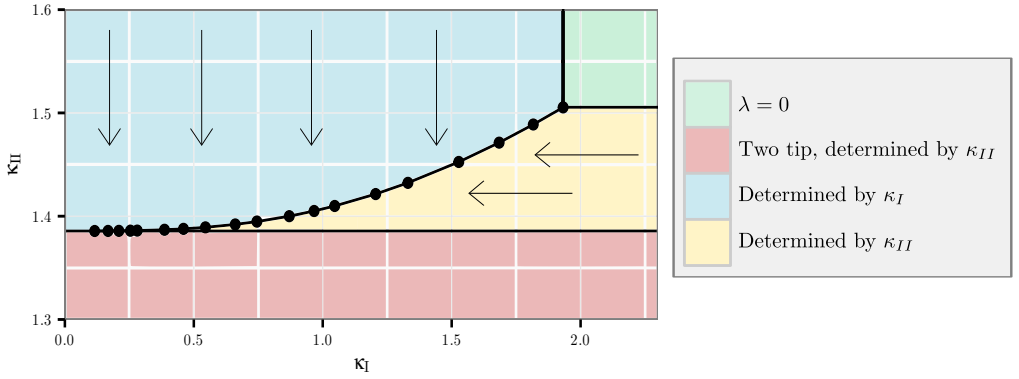
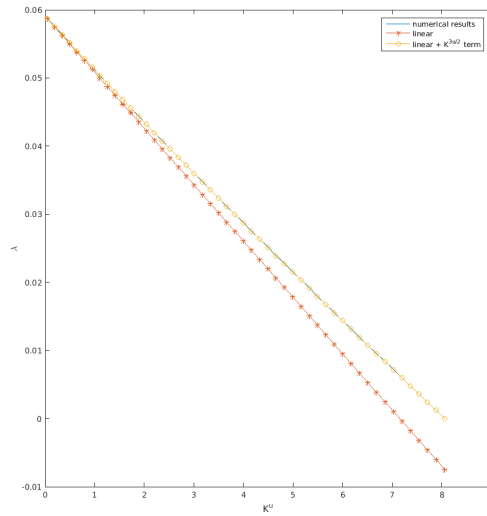


FIGURE 8. Some of the numerical results for the two tip problem. Having  $\kappa_I \neq 0$  at  $\xi = 0$  and  $L \neq 0$  is unphysical, but is what is found numerically. We can recover the physical solution by increasing  $\lambda$  for fixed  $L$  until  $\kappa_I = 0$ .

vary much with  $\lambda_0$ , and that given a reference  $H'$ , one can construct  $G'$  with relative ease.

At this point, I would like to construct another contrived formulae for the two tip problem. Then I would like to plot a graph of  $\kappa_I$  against  $\kappa_{II}$  in the full fluid problem.

FIGURE 9. The results of extrapolating to  $\kappa_I = 0$ FIGURE 10. Given values  $(\kappa_I, \kappa_{II})$ , this graph determines which fracture regime occurs and so how  $\lambda$  and/or  $L$  should be calculated.FIGURE 11. The formula valid for all  $\kappa_I$

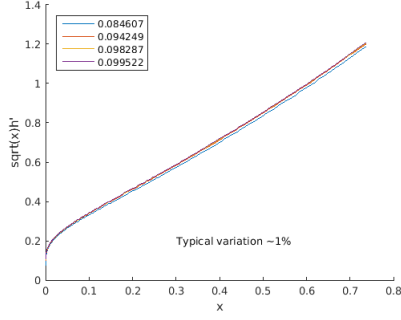
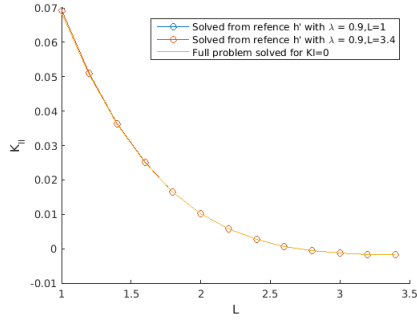


FIGURE 12. Demonstrating the decoupling of fluid and solid fracture

FIGURE 13. Reconstructing the full solution given a reference  $H'$ 

This provides a guide of when it is appropriate to take the single tip, and when it is appropriate to take the double tip.

---

$a/d$	$M = 4$	$M = 8$	Callan <i>et al.</i>
0.1	1.56905	1.56	1.56904
0.3	1.50484	1.504	1.50484
0.55	1.39128	1.391	1.39131
0.7	1.32281	10.322	1.32288
0.913	1.34479	100.351	1.35185

---

TABLE 1. Values of  $kd$  at which trapped modes occur when  $\rho(\theta) = a$ 

## 6. Citations and references

All papers included in the References section must be cited in the article, and vice versa. Citations should be included as, for example “It has been shown (Rogallo 1981) that...” (using the `\citep` command, part of the natbib package) “recent work by Dennis (1985)...” (using `\citet`). The natbib package can be used to generate citation variations, as shown below.

`\citet[pp. 2-4]{Hwang70}`:

Hwang & Tuck (1970, pp. 2-4)

`\citep[p. 6]{Worster92}`:

(Worster 1992, p. 6)

`\citep[see][]{Koch83, Lee71, Linton92}`:

(see Koch 1983; Lee 1971; Linton & Evans 1992)

`\citep[see][p. 18]{Martin80}`:

(see Martin 1980, p. 18)

`\citep{Brownell104, Brownell107, Ursell150, Wijngaarden68, Miller91}`:

(Brownell & Su 2004, 2007; Ursell 1950; van Wijngaarden 1968; Miller 1991)

The References section can either be built from individual `\bibitem` commands, or can be built using BibTeX. The BibTeX files used to generate the references in this document can be found in the zip file at <http://journals.cambridge.org/data/relatedlink/jfm-ifc.zip>.

Where there are up to ten authors, all authors’ names should be given in the reference list. Where there are more than ten authors, only the first name should appear, followed by *et al.*

Acknowledgements should be included at the end of the paper, before the References section or any appendices, and should be a separate paragraph without a heading. Several anonymous individuals are thanked for contributions to these instructions.

## Appendix A

This appendix contains sample equations in the JFM style. Please refer to the L<sup>A</sup>T<sub>E</sub>X source file for examples of how to display such equations in your manuscript.

$$(\nabla^2 + k^2)G_s = (\nabla^2 + k^2)G_a = 0 \quad (\text{A } 1)$$

$$\nabla \cdot \mathbf{v} = 0, \quad \nabla^2 P = \nabla \cdot (\mathbf{v} \times \mathbf{w}). \quad (\text{A } 2)$$

$$G_s, G_a \sim 1/(2\pi) \ln r \quad \text{as} \quad r \equiv |P - Q| \rightarrow 0, \quad (\text{A } 3)$$

$$\left. \begin{aligned} \frac{\partial G_s}{\partial y} &= 0 \quad \text{on} \quad y = 0, \\ G_a &= 0 \quad \text{on} \quad y = 0, \end{aligned} \right\} \quad (\text{A } 4)$$

$$-\frac{1}{2\pi} \int_0^\infty \gamma^{-1} [\exp(-k\gamma|y-\eta|) + \exp(-k\gamma(2d-y-\eta))] \cos k(x-\xi) t \, dt, \quad 0 < y, \quad \eta < d, \quad (\text{A } 5)$$

$$\gamma(t) = \begin{cases} -i(1-t^2)^{1/2}, & t \leq 1 \\ (t^2-1)^{1/2}, & t > 1. \end{cases} \quad (\text{A } 6)$$

$$-\frac{1}{2\pi} \int_0^\infty B(t) \frac{\cosh k\gamma(d-y)}{\gamma \sinh k\gamma d} \cos k(x-\xi) t \, dt$$

$$G = -\frac{1}{4}i(H_0(kr) + H_0(kr_1)) - \frac{1}{\pi} \int_0^\infty \frac{e^{-k\gamma d}}{\gamma \sinh k\gamma d} \cosh k\gamma(d-y) \cosh k\gamma(d-\eta) \quad (\text{A } 7)$$

Note that when equations are included in definitions, it may be suitable to render them in line, rather than in the equation environment:  $\mathbf{n}_q = (-y'(\theta), x'(\theta))/w(\theta)$ . Now  $G_a = \frac{1}{4}Y_0(kr) + \widetilde{G}_a$  where  $r = \{[x(\theta) - x(\psi)]^2 + [y(\theta) - y(\psi)]^2\}^{1/2}$  and  $\widetilde{G}_a$  is regular as  $kr \rightarrow 0$ . However, any fractions displayed like this, other than  $\frac{1}{2}$  or  $\frac{1}{4}$ , must be written on the line, and not stacked (ie 1/3).

$$\begin{aligned} \frac{\partial}{\partial n_q} \left( \frac{1}{4} Y_0(kr) \right) &\sim \frac{1}{4\pi w^3(\theta)} [x''(\theta)y'(\theta) - y''(\theta)x'(\theta)] \\ &= \frac{1}{4\pi w^3(\theta)} [\rho'(\theta)\rho''(\theta) - \rho^2(\theta) - 2\rho'^2(\theta)] \quad \text{as} \quad kr \rightarrow 0. \end{aligned} \quad (\text{A } 8)$$

$$\frac{1}{2}\phi_i = \frac{\pi}{M} \sum_{j=1}^M \phi_j K_{ij}^a w_j, \quad i = 1, \dots, M, \quad (\text{A } 9)$$

where

$$K_{ij}^a = \begin{cases} \partial G_a(\theta_i, \theta_j) / \partial n_q, & i \neq j \\ \partial \widetilde{G}_a(\theta_i, \theta_i) / \partial n_q + [\rho'_i \rho''_i - \rho_i^2 - 2\rho_i'^2] / 4\pi w_i^3, & i = j. \end{cases} \quad (\text{A } 10)$$

$$\rho_l = \lim_{\zeta \rightarrow Z_l^-(x)} \rho(x, \zeta), \quad \rho_u = \lim_{\zeta \rightarrow Z_u^+(x)} \rho(x, \zeta) \quad (\text{A } 11a, b)$$

$$(\rho(x, \zeta), \phi_{\zeta\zeta}(x, \zeta)) = (\rho_0, N_0) \quad \text{for} \quad Z_l(x) < \zeta < Z_u(x). \quad (\text{A } 12)$$

$$\tau_{ij} = (\overline{u_i u_j} - \overline{u_i} \overline{u_j}) + (\overline{u_i u_j^{SGS}} + \overline{u_i^{SGS} u_j}) + \overline{u_i^{SGS} u_j^{SGS}}, \quad (\text{A } 13a)$$

$$\tau_j^\theta = (\overline{u_j \theta} - \overline{u_j} \overline{\theta}) + (\overline{u_j \theta^{SGS}} + \overline{u_j^{SGS} \theta}) + \overline{u_j^{SGS} \theta^{SGS}}. \quad (\text{A } 13b)$$

$$\mathbf{Q}_C = \begin{bmatrix} -\omega^{-2}V'_w & -(\alpha^t\omega)^{-1} & 0 & 0 & 0 \\ \frac{\beta}{\alpha\omega^2}V'_w & 0 & 0 & 0 & i\omega^{-1} \\ i\omega^{-1} & 0 & 0 & 0 & 0 \\ iR_\delta^{-1}(\alpha^t + \omega^{-1}V''_w) & 0 & -(i\alpha^t R_\delta)^{-1} & 0 & 0 \\ \frac{i\beta}{\alpha\omega}R_\delta^{-1}V''_w & 0 & 0 & 0 & 0 \\ (i\alpha^t)^{-1}V'_w & (3R_\delta^{-1} + c^t(i\alpha^t)^{-1}) & 0 & -(\alpha^t)^{-2}R_\delta^{-1} & 0 \end{bmatrix}. \quad (\text{A } 14)$$

$$\boldsymbol{\eta}^t = \hat{\boldsymbol{\eta}}^t \exp[i(\alpha^t x_1^t - \omega t)], \quad (\text{A } 15)$$

where  $\hat{\boldsymbol{\eta}}^t = \mathbf{b} \exp(i\gamma x_3^t)$ .

$$\text{Det}[\rho\omega^2\delta_{ps} - C_{pqrs}^t k_q^t k_r^t] = 0, \quad (\text{A } 16)$$

$$\langle k_1^t, k_2^t, k_3^t \rangle = \langle \alpha^t, 0, \gamma \rangle \quad (\text{A } 17)$$

$$\mathbf{f}(\theta, \psi) = (g(\psi) \cos \theta, g(\psi) \sin \theta, f(\psi)). \quad (\text{A } 18)$$

$$f(\psi_1) = \frac{3b}{\pi[2(a+b\cos\psi_1)]^{3/2}} \int_0^{2\pi} \frac{(\sin\psi_1 - \sin\psi)(a+b\cos\psi)^{1/2}}{[1-\cos(\psi_1-\psi)](2+\alpha)^{1/2}} dx, \quad (\text{A } 19)$$

$$\begin{aligned} g(\psi_1) = & \frac{3}{\pi[2(a+b\cos\psi_1)]^{3/2}} \int_0^{2\pi} \left( \frac{a+b\cos\psi}{2+\alpha} \right)^{1/2} \left\{ f(\psi)[(\cos\psi_1 - b\beta_1)S + \beta_1 P] \right. \\ & \times \frac{\sin\psi_1 - \sin\psi}{1 - \cos(\psi_1 - \psi)} + g(\psi) \left[ \left( 2 + \alpha - \frac{(\sin\psi_1 - \sin\psi)^2}{1 - \cos(\psi - \psi_1)} - b^2\gamma \right) S \right. \\ & \left. \left. + \left( b^2 \cos\psi_1 \gamma - \frac{a}{b} \alpha \right) F\left(\frac{1}{2}\pi, \delta\right) - (2 + \alpha) \cos\psi_1 E\left(\frac{1}{2}\pi, \delta\right) \right] \right\} d\psi, \end{aligned} \quad (\text{A } 20)$$

$$\alpha = \alpha(\psi, \psi_1) = \frac{b^2[1 - \cos(\psi - \psi_1)]}{(a + b\cos\psi)(a + b\cos\psi_1)}, \quad \beta - \beta(\psi, \psi_1) = \frac{1 - \cos(\psi - \psi_1)}{a + b\cos\psi}. \quad (\text{A } 21)$$

$$\left. \begin{aligned} H(0) &= \frac{\epsilon \bar{C}_v}{\tilde{v}_T^{1/2}(1-\beta)}, \quad H'(0) = -1 + \epsilon^{2/3} \bar{C}_u + \epsilon \hat{C}'_u; \\ H''(0) &= \frac{\epsilon u_*^2}{\tilde{v}_T^{1/2} u_P^2}, \quad H'(\infty) = 0. \end{aligned} \right\} \quad (\text{A } 22)$$

LEMMA 1. Let  $f(z)$  be a trial Batchelor (1971, pp. 231–232) function defined on  $[0, 1]$ . Let  $\Lambda_1$  denote the ground-state eigenvalue for  $-\text{d}^2g/\text{d}z^2 = \Lambda g$ , where  $g$  must satisfy  $\pm \text{d}g/\text{d}z + \alpha g = 0$  at  $z = 0, 1$  for some non-negative constant  $\alpha$ . Then for any  $f$  that is not identically zero we have

$$\frac{\alpha(f^2(0) + f^2(1)) + \int_0^1 \left( \frac{\text{d}f}{\text{d}z} \right)^2 \text{d}z}{\int_0^1 f^2 \text{d}z} \geq \Lambda_1 \geq \left( \frac{-\alpha + (\alpha^2 + 8\pi^2\alpha)^{1/2}}{4\pi} \right)^2. \quad (\text{A } 23)$$

COROLLARY 1. *Any non-zero trial function  $f$  which satisfies the boundary condition  $f(0) = f(1) = 0$  always satisfies*

$$\int_0^1 \left( \frac{df}{dz} \right)^2 dz. \quad (\text{A } 24)$$

## REFERENCES

- BATCHELOR, G. K. 1971 Small-scale variation of convected quantities like temperature in turbulent fluid. part 1. general discussion and the case of small conductivity. *J. Fluid Mech.* **5**, 113–133.
- BROWNELL, C. J. & SU, L. K. 2004 Planar measurements of differential diffusion in turbulent jets. *AIAA Paper 2004-2335*.
- BROWNELL, C. J. & SU, L. K. 2007 Scale relations and spatial spectra in a differentially diffusing jet. *AIAA Paper 2007-1314*.
- DENNIS, S. C. R. 1985 Compact explicit finite difference approximations to the Navier–Stokes equation. In *Ninth Intl Conf. on Numerical Methods in Fluid Dynamics* (ed. Soubbaramayer & J. P. Boujot), *Lecture Notes in Physics*, vol. 218, pp. 23–51. Springer.
- HWANG, L.-S. & TUCK, E. O. 1970 On the oscillations of harbours of arbitrary shape. *J. Fluid Mech.* **42**, 447–464.
- KOCH, W. 1983 Resonant acoustic frequencies of flat plate cascades. *J. Sound Vib.* **88**, 233–242.
- LEE, J.-J. 1971 Wave-induced oscillations in harbours of arbitrary geometry. *J. Fluid Mech.* **45**, 375–394.
- LINTON, C. M. & EVANS, D. V. 1992 The radiation and scattering of surface waves by a vertical circular cylinder in a channel. *Phil. Trans. R. Soc. Lond.* **338**, 325–357.
- MARTIN, P. A. 1980 On the null-field equations for the exterior problems of acoustics. *Q. J. Mech. Appl. Maths* **33**, 385–396.
- MILLER, P. L. 1991 Mixing in high schmidt number turbulent jets. PhD thesis, California Institute of Technology.
- ROGALLO, R. S. 1981 Numerical experiments in homogeneous turbulence. *Tech. Rep.* 81835. NASA Tech. Mem.
- URSELL, F. 1950 Surface waves on deep water in the presence of a submerged cylinder i. *Proc. Camb. Phil. Soc.* **46**, 141–152.
- VAN WIJNGAARDEN, L. 1968 On the oscillations near and at resonance in open pipes. *J. Engng Maths* **2**, 225–240.
- WORSTER, M. G. 1992 The dynamics of mushy layers. In *Interactive dynamics of convection and solidification* (ed. S. H. Davis, H. E. Huppert, W. Muller & M. G. Worster), pp. 113–138. Kluwer.